NATURE|Vol 448|19 July 2007|doi:10.1038/nature06080

The quest for the quark–gluon plasma

Peter Braun-Munzinger[1] & Johanna Stachel[2]

High-energy collisions between heavy nuclei have in the past 20 years provided multiple indications of a deconfined phase of matter that exists at phenomenally high temperatures and pressures. This 'quark–gluon plasma' is thought to have permeated the first microseconds of the Universe. Experiments at the Large Hadron Collider should consolidate the evidence for this exotic medium's existence, and allow its properties to be characterized.

Shortly after the idea of asymptotic freedom — that the interaction between quarks, which is strong at large separations, weakens as the quarks get closer to one another — was introduced by David Gross and Frank Wilczek[1] and David Politzer[2], two groups[3,4] realized independently that it has a fascinating consequence. When temperatures or densities become very high, strongly interacting quarks and gluons become free and transform themselves into a new, deconfined phase of matter, for which the term 'quark–gluon plasma' was coined. We ourselves live at low densities and temperatures, in the normal world of hadronic matter, where quarks and gluons are confined to the size of hadrons. But at its origin, the Universe was a fireball of much higher density and temperature. At times from the electroweak phase transition — some 10 picoseconds after the Big Bang, and lasting for 10 microseconds — it is thought to have taken the form of a quark–gluon plasma. Here, we review the current state of knowledge of this peculiar phase of matter, and outline how the Large Hadron Collider (LHC) should further our understanding of it.

Transition temperature

Various simple estimates lead to a critical temperature for the transition between the familiar, confined hadronic phase of matter and the deconfined, plasma phase of the order of 100 MeV. (In this review, we use the kT unit system, in which all temperatures (T) are multiplied by Boltzmann's constant $k = 8.617 \times 10^{-5}$ eV K^{-1} to express them in more convenient energy units; for reference, a temperature of 100 MeV is somewhat more than 1 trillion kelvin, at 1.16×10^{12} K.) In detailed investigations of hadronic matter, Rolf Hagedorn[5] discovered in the 1960s a limiting temperature for hadronic systems of around the π-meson mass of 140 MeV. It turns out that this temperature is nothing other than the critical temperature for the deconfinement phase transition.

With the advance of solving quantum chromodynamics — the quantum field theory of the strong interaction — on a space-time lattice, more accurate values have become available for the transition temperature. The most readily calculable values are those for a zero net baryon density (that is, no difference between baryon and antibaryon densities). For instance, researchers obtained a temperature[6] of 173 MeV with a systematic error of about 10% for a system involving the two light quark flavours (up and down) and one heavier quark flavour (strange). Very recently, higher values in the vicinity of 190 MeV have been quoted. The reason for the variations is that the lattice energy units have been normalized differently: now, the calculations use quantities that involve heavy bottom quarks, whereas in the past they used the mass of the ρ meson, which contains only the light up and down quarks (see page 270). There is currently a lively debate (see, for example, ref. 7) about the most accurate way to calculate the transition temperature.

Extending lattice quantum chromodynamics into the regime of non-zero net baryon density has met with great technical difficulties. Results[8–10] have become available indicating that the transition temperature drops moderately with increasing density. Going a third of the way from zero net density to the density of atomic nuclei, it drops by 2–3% — not very much. The critical energy density for the phase transition is 0.7 ± 0.2 GeV fm^{-3} (ref. 6). This energy density is about five times that of nuclear matter.

Towards the nuclear fireball

Since the early 1980s, collisions of heavy atomic nuclei at as large energies as possible have been seen as the ideal way to probe these harsh conditions of extremely high temperature and density. To be able to talk about thermodynamic phases, phase transitions, temperatures and so on, the system under consideration must behave like 'matter', not like individual elementary particles or a group of elementary particles. That implies two things. First, the system must consist of a large number of particles (thousands or, better, tens of thousands). Second, it needs to reach local equilibrium, at least approximately, so that variables such as temperature, pressure, energy and entropy density can be defined, and so that thermodynamic relations between those quantities (the equation of state, the speed of sound) can be investigated. This means that the system's lifetime must be significantly larger than the inverse rate of interactions, so that at least a few (order of magnitude five) interactions occur for each constituent, driving the system towards equilibrium.

Collisions of protons (or electrons) produce too few particles to fulfil these conditions. But we know now that collisions between nuclei create enough particles that, if the energy is high enough, they do indeed create a fireball of interacting quarks and gluons above the temperature needed for the phase transition into deconfinement. This fireball quickly expands and cools, until it rehadronizes on passing the deconfinement temperature again. The hugely energetic fireball created in the aftermath of the Big Bang had cooled sufficiently for protons and neutrons (and other confined, but unstable, hadrons) to form after about 10^{-5} s. The fireball created in a nuclear collision in the laboratory contains much less energy, and so is much shorter-lived than that after the Big Bang: after only about 10^{-22} s, the quark–gluon plasma phase of the fireball transforms back to hadronic matter.

Collisions of atomic nuclei have been studied for about 20 years at sufficiently high energies to cross into the deconfined phase. Experimental programmes started simultaneously in late 1986 at the Alternating Gradient Synchrotron at the Brookhaven National Laboratory (BNL) in Upton, New York, and at the Super Proton Synchrotron (SPS)

[1]Gesellschaft für Schwerionenforschung, Planckstr. 1, D 64291, Darmstadt, Germany and Technische Universität Darmstadt. [2]Physikalisches Institut, Universität Heidelberg, Philosophenweg 12, D69120 Heidelberg, Germany.

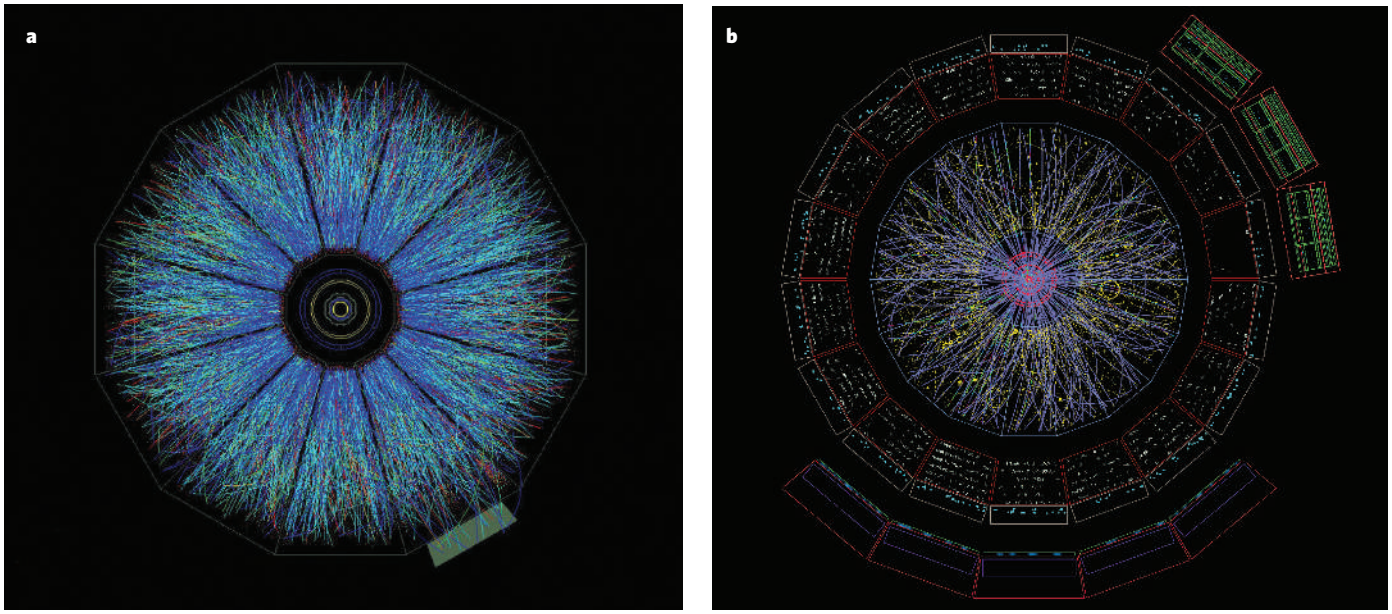

Figure 1 | Fireball remnants. a, Charged particles from a central gold–gold collision at RHIC, recorded by the time projection chamber of the STAR experiment. Colours represent the level of ionization deposited in the detector, with red equating to high values and blue to low values. **b**, A simulation of a central lead–lead collision — just a one-degree slice in polar angle is shown — in the central barrel of the ALICE experiment at the LHC. **Images courtesy of the STAR and ALICE collaborations.**

at CERN. At both facilities, collisions were studied initially with light atomic nuclei (up to silicon and sulphur, with mass numbers of 28 and 32, respectively) and, from the early 1990s, also with heavy nuclei such as gold (mass number 197) and the most abundant isotope of lead (208). For these heavy colliding nuclei, BNL has reached energies in the centre-of-mass system of close to 1,000 GeV, and CERN has reached 3,600 GeV (corresponding to a centre-of-mass energy per colliding nucleon pair, written as $\sqrt{s_{NN}}$, of 4.6 and 17.2 GeV, respectively). At least for the CERN energy regime, enough evidence was gathered to conclude that a new state of matter had been created in these collisions[11,12].

At the same time, a huge next step was being taken. At BNL, a dedicated new accelerator, the Relativistic Heavy-Ion Collider (RHIC), went into operation, servicing four experiments, called BRAHMS, PHENIX, PHOBOS and STAR. At RHIC, heavy nuclei such as gold collide at a relativistic centre-of-mass energy of 40,000 GeV ($\sqrt{s_{NN}} = 200$ GeV). This higher collision energy means a much larger and hotter fireball than had previously been possible (Fig. 1). Data from the first three years of running at RHIC are summarized in refs 13–16, and more recent data can be found in ref. 17.

An even braver new world will come about with the start of operations at the LHC, in which nuclei with masses up to that of lead will be able to collide at a centre-of-mass energy of 1,150 TeV ($\sqrt{s_{NN}} = 5.5$ TeV). This is a huge step in collision energy, about 30 times more than that of RHIC and, at about 0.18 mJ, the first really 'macroscopic' energy to be investigated. The fireball is expected to contain tens of thousands of gluons and quarks, and its temperature should exceed the critical temperature for the deconfinement phase transition several times over. This huge increase in energy should allow the unambiguous identification and characterization of the quark–gluon plasma.

A fireball in chemical equilibrium

As mentioned earlier, one of the crucial questions to be addressed in considering ultra-relativistic collisions between nuclei is the extent to which matter is formed in the fireball. There are two important sets of observations that support the idea of a matter-like fireball. The first concerns the fact that the fireball yields hadrons that are in chemical equilibrium, forming a statistical ensemble. Hadron yields have been studied with high precision in nuclear collisions at the energies used in

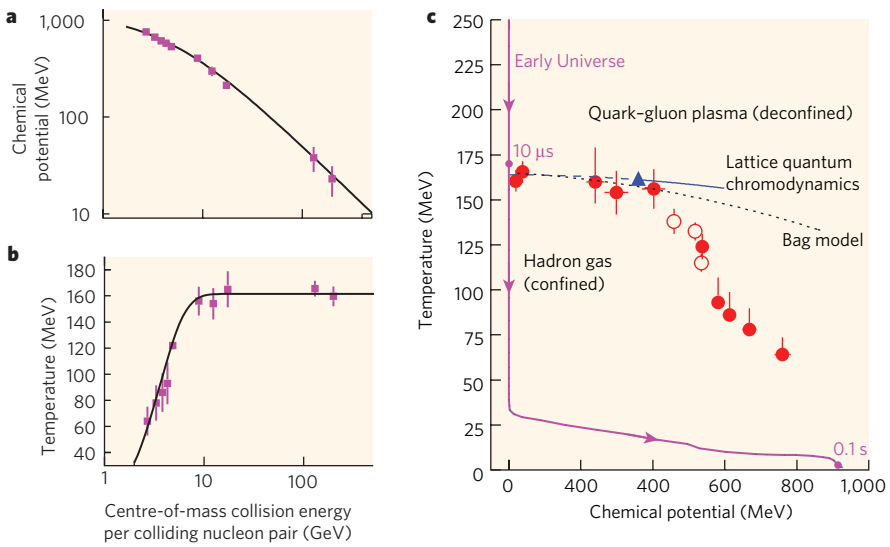

Figure 2 | Equilibrium parameters of the fireball. The energy dependence of chemical potential (**a**) and temperature (**b**), determined from a statistical analysis of hadron yields[18]. The temperature plateau at high collision energies suggests the presence of a phase boundary. Pink squares are results of individual experiments. **c**, The phase diagram of strongly interacting matter: the data points are obtained as in **a** and **b**. The evolution of the early Universe is shown, as are theoretical expectations such as from lattice quantum chromodynamics (blue line) and the bag model (dotted line) for the phase boundary between confined and deconfined matter. Red filled circles are from analysis of midrapidity data. Open circles are from analysis of 4π data. Blue triangle is possible position of a critical endpoint. **Figure reproduced, with permission, from ref. 18.**

the Alternating Gradient Synchrotron, SPS and RHIC. These yields can be described by assuming that all hadrons are formed only when the fireball reaches a specific equilibrium temperature, volume and baryon chemical potential (a measure of the energy change brought about by the addition of one more baryon to the system). Under these conditions, the hadron yields can be characterized in relatively simple terms by the thermodynamic grand-canonical ensemble or, in the special case of small particle numbers, by the canonical ensemble. Such conditions are dubbed the 'chemical freeze-out' scenario, in analogy to the production of bound particles as the early Universe cooled. Detailed analyses of the freeze-out can be found in refs 18 and 19, and a comprehensive review in ref. 20.

Importantly, the energies attained in the SPS and RHIC are also high enough to produce particles containing several strange quarks, including the Ω and $\bar{\Omega}$ baryons. Yields of these baryons agree very well with chemical-equilibrium calculations, and are much higher than in proton–proton collisions. The interpretation is that in heavy-ion collisions, the chemical freeze-out is caused by the quark–gluon plasma and its transition to normal matter, whereas this plasma is absent in collisions between protons.

With increasing centre-of-mass collision energy, the chemical potential decreases smoothly, so new baryons and antibaryons can be created with increasing ease (Fig. 2a). By contrast, although the temperature increases strongly at first, it plateaus rather abruptly near $\sqrt{s_{NN}} = 10$ GeV, at a value slightly higher than 160 MeV (Fig. 2b). This plateau supports Hagedorn's limiting-temperature hypothesis[5], and strongly suggests that a boundary — the phase boundary — is reached at a critical collision energy. Beyond that energy, all additional energy goes into heating the quark–gluon plasma which, in turn, cools again and freezes out at the phase boundary (critical temperature).

If the temperature of the collision fireball is plotted against its chemical potential, with one entry for each energy investigated, a phase diagram can be constructed for the strongly interacting matter contained within it (Fig. 2c). What emerges can be compared to various predictions of the position of the phase boundary taken[8–10] from lattice quantum chromodynamics and[21] from a simple 'bag model' of quarks' confinement into hadrons. For chemical potentials of less than about 400 MeV — corresponding to the critical energy discussed above — the temperatures and chemical potentials determined from the measured hadron yields coincide, within about 10 MeV uncertainty, with the phase boundary as determined from lattice quantum chromodynamics calculations. When the phase boundary is reached, all further points follow it — hadrons cannot be formed in the quark–gluon plasma, only as the plasma rehadronizes.

But could this just be coincidence? What mechanism enforces equilibrium at the phase boundary? Collision rates and the timescales of fireball expansion in the hadronic phase[22] imply that, at the energies used in the SPS and RHIC, equilibrium cannot be established in the hadronic medium. Rather, it is the phase transition between deconfined and confined matter that ensures chemical equilibrium through multi-particle collisions during hadronization. Alternatively, the plateau can be interpreted to arise[23,24] from the filling of phase space during hadronization. In either case, all current interpretations of the observed phenomena relate the chemical variables directly to the phase boundary. This implies that a fundamental parameter of quantum chromodynamics — namely the critical temperature for the deconfinement phase transition — has been determined experimentally to be close to 160 MeV, for small values of chemical potential.

This interpretation will be tested directly by experiments at the LHC. If the plateau phenomenon holds, as is to be expected from the above considerations, then the particle yields measured at LHC energy should, except for an overall volume parameter, agree closely with those measured at the much smaller RHIC energy. That would lend strong support to a phase boundary as the limiting agent.

The observed equilibrium is a strong indication that a matter-like medium is produced in high-energy collisions between nuclei. In collisions among particles such as leptons or nucleons, such equilibrium is not observed, at least not at the energies at which particles containing strange quarks can be produced[20], and hence no medium is formed. We finally note that, as is evident from Fig. 2c, in heavy-ion collisions the chemical freeze-out temperature is not universal but instead varies strongly at large values of the chemical potential. This implies that the properties of the medium change with energy, indicating a transition to a baryon-rich medium at low energies.

The phase transition at low baryon density is probably of the cross-over type[25]. General considerations, as well as results from lattice quantum chromodynamics, suggest the possibility of a first-order phase transition at higher baryon densities with a corresponding critical end-point as sketched in Fig. 2c. Experiments to search for the critical point are planned at the SPS, RHIC and the future Facility for Antiproton and Ion Research (FAIR) at the heavy-ion research centre GSI in Darmstadt, Germany.

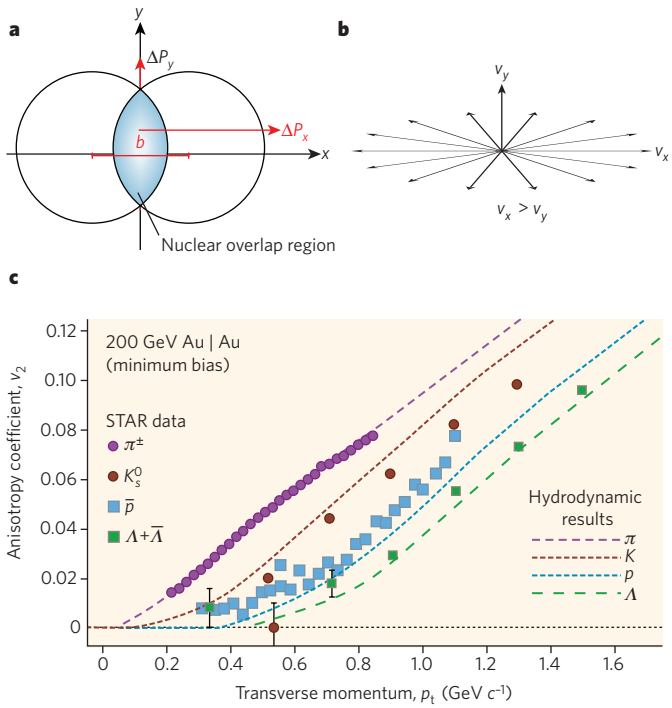

Figure 3 | Geometry of matter during a nuclear collision. a, The nuclear overlap region for semi-central collisions. Early in the collision, the pressure gradient is large in the plane of the collision, *x*. After some time, the large pressure gradient leads to a larger expansion velocity (v_x) in this direction (**b**). The expansion velocity profile in the *x*–*y* plane leads to highly asymmetrical particle emission, with azimuthal anisotropies in momenta perpendicular to the beam (p_t) of various particles. **c**, The distribution of these momenta can be quantified by a Fourier decomposition and parametrized by the second Fourier coefficient $v_2 = \langle\cos 2\varphi\rangle$ — also called the 'elliptical flow'[56–58] — in which the angle φ is measured relative to the direction of impact: higher transverse momenta are recorded for particles emerging in the reaction plane, whereas much lower momenta are observed perpendicular to the reaction plane. As a consequence, the v_2 coefficients are large and show a characteristic p_t dependence. Data for π mesons, *K* mesons, antiprotons ($\bar{p}$) and Λ baryons (with masses mc^2 of about 140, 495, 940 and 1,115 MeV, respectively) agree very well in their mass- and p_t-dependence with predictions[59–61] made with relativistic hydrodynamics and an equation of state determined by weakly interacting quarks and gluons. Although the data are not very sensitive to the particular equation of state used, equations of state based exclusively on hadrons do not lead to a satisfactory description of the data. The data shown are from the STAR experiment at RHIC[62]. **Part c reproduced, with permission, from ref. 62.**

Hydrodynamic expansion and cooling

If matter is formed in the moments after a nuclear collision, hydrodynamic flow effects should be seen owing to the strong pressure gradients present in it. At ultra-relativistic energies, two colliding nuclei are highly

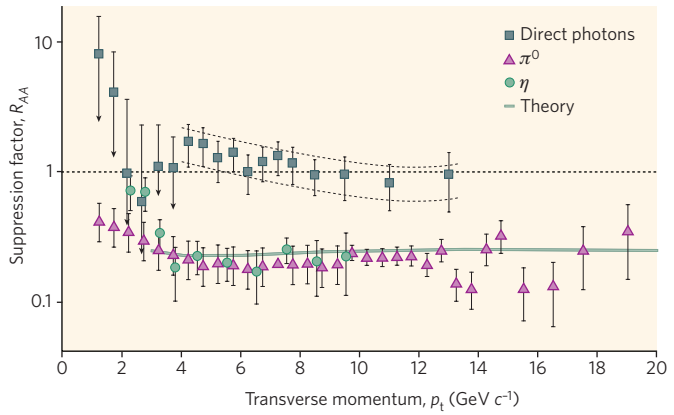

Figure 4 | Preliminary PHENIX results for the suppression factor R_{AA} out to high p_t for π^0 and η mesons. R_{AA} is the ratio of the number of events at different values of p_t for gold–gold collisions normalized to the number of events in proton–proton collisions, scaled by the number of collisions. The suppression of the gold–gold spectrum at high p_t is further evidence for the presence of a hot, dense medium on which jet partons scatter and lose momentum. Bars indicate statistical error. The dotted line at $R_{AA} = 1$ is the expected result when the photon spectrum is unmodified. A theoretical spectrum[63] is also shown, calculated under the assumptions that the precursor parton of the jet loses energy by radiation, and that the medium can be modelled as dense gluon gas. It agrees well with the experimental data. The results for photons produced directly in gold–gold and proton–proton collisions are also shown. These show no suppression; this is consistent with the idea of a gluon gas, as photons do not participate in strong interactions. Figure courtesy of the PHENIX collaboration.

Lorentz-contracted — at the RHIC energy by a factor of 100, at the LHC energy by a factor of 2,700. Consequently, the collision is very quick, lasting around 10^{-25} s. The geometry of the matter immediately after the collision is sketched in Fig. 3a; with increasing impact, b, the overlap zone becomes more and more aspherical in the plane perpendicular to the axis of the colliding beams. It attains an almond-like shape with a typical size in the perpendicular plane determined by the dimensions of the nuclei involved (the diameter of a lead nucleus is about 14 fm), whereas the extension in beam direction cannot be greater than the speed of light multiplied by the collision time — less than 1 fm.

This highly asymmetrical zone evolves by collisions between its constituents (quarks and gluons) until, after a time of about 1 fm c^{-1}, equilibrium is reached and a highly compressed, but still very asymmetrical, fireball is formed. The details of this initial phase are not well understood, but might involve highly coherent configurations of colour fields, generated by a 'colour glass condensate'[26], large fluctuations of which are thought to lead to extremely rapid equilibrium. Irrespective of the details of this highly complex evolution, some ground rules are clear if equilibrium is reached in a short enough time that the shape of the fireball remains essentially unchanged from the initial geometric overlap zone. In this case, the fireball's further evolution should be governed by the laws of relativistic hydrodynamics for a system with very strong pressure gradients, as well as by the equation of state that connects the variables such as volume, temperature and chemical potential that characterize the medium. When the original spatial correlation is transformed into a correlation in momentum (or velocity) space, this implies a very asymmetrical particle emission in the plane perpendicular to the axis of the colliding beams (Fig. 3b). The earlier the equilibrium, and with it the beginning of the hydrodynamic evolution, the larger the anisotropies will be.

What observations are to be expected if the fireball really does expand hydrodynamically, with a unique collective velocity for each fluid cell in the system? The transverse momenta (p_t) of the emitted particles are connected to the fluid velocity via $p_t = m\beta_f\gamma_f$ (with $\gamma_f = 1/\sqrt{1-\beta_f}$), in which m is the mass of the particle, β_f is the relativistic fluid velocity and γ_f is its Lorentz factor, and a characteristic mass-dependent flow pattern arises. The resulting mass ordering in the anisotropy coefficients (v_2) agrees closely with the experimental observations (Fig. 3c). The large anisotropy coefficients confirm the idea that the fireball reaches equilibrium rapidly.

This dramatic and unexpected success is the second strong pillar supporting the idea that ultra-relativistic nuclear collisions produce a collectively expanding medium in thermal equilibrium. We note here that the hydrodynamic calculations with which the experimental data are in such good agreement assume that fluid flow is non-viscous. When added to the hydrodynamic equations, even small viscosity destroys the agreement between data and calculations. Researchers have thus concluded that the matter made in the RHIC fireball is probably close to an ideal fluid[27–29].

If the fireball really does behave hydrodynamically at top RHIC energy, then the elliptical flow data from the LHC should be similar to those from RHIC. The anticipated much greater number of particles produced in each collision could be used to measure flow precisely for many types of particle. That could in turn allow the equation of state of the matter and its transport coefficients (such as viscosity) to be pinned down. Alternatively, as still argued by some authors[30], the flow pattern observed at RHIC is due to a cancellation between unusual initial conditions of the fireball owing to a colour glass condensate on the one hand and an imperfect thermal equilibrium on the other. If that is so, or if viscous effects do play a part, then the LHC data on elliptical flow could reach much larger values. In any case, the very large energy step when going from RHIC to the LHC should lead to important, and urgently needed, new information on the physics of the quark–gluon plasma.

An opaque matter

In collisions of heavy nuclei, hard scattering events — those with high momentum transfer — between the constituent 'partons' (quarks and gluons) liberated are expected to occur just as in collisions between protons. The number of such events, however, will scale with the number of individual proton–proton collisions for a given collision geometry: for head-on collisions of two equal nuclei of mass number A, the number of

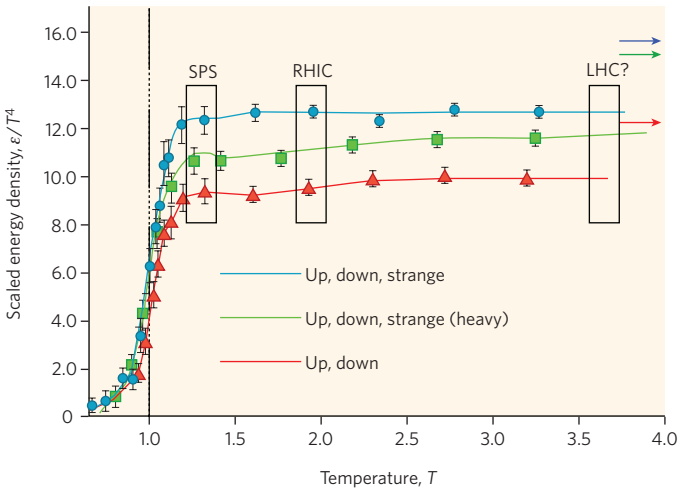

Figure 5 | Scaled energy density ε/T^4 as a function of the temperature calculated in lattice quantum chromodynamics[6]. For an ideal gas, the energy density is proportional to the fourth power of the temperature with the proportionality constant containing the number of degrees of freedom. The strong increase near the critical temperature (T_c, vertical line) indicates that the system is not only heated but that something dramatic happens: it undergoes a phase transition from hadronic matter to quark–gluon plasma with a corresponding large increase in the number of degrees of freedom. Above T_c, the quark–gluon plasma is only heated such that ε/T^4 is constant. The three lines are calculations for two light quark flavours (only up and down; red), three equally light flavours (up, down and strange; blue) and the most realistic case of two light flavours (up and down) and one more massive (strange) flavour (green). Coloured arrows show the expected values of scaled energy density at the Stefan-Boltzman limit. The regions labelled by accelerator facilities indicate maximum initial temperatures reached there. Figure reproduced, with permission, from ref. 65.

events will scale as $A^{4/3}$. Individual collisions between protons are thought to occur independently of each other, and their number can be computed from the distributions of the nuclear densities, the nuclear overlap for a given impact and the inelastic proton–proton cross-section.

Collisions of nuclei differ from collisions between protons in that the hard scattered partons may traverse the quark–gluon plasma before or during their hadronization into a jet. Jets are characteristic of collisions between protons in which two constituent partons scatter and recede from each other with a significant fraction of the initial beam momentum. In the plane transverse to the beams, the momenta are large and opposite in direction. The two scattered partons hadronize mainly into mesons that are emitted in a cone — the jet — around the direction of parton momentum. It was realized very early[31] that the quark–gluon plasma could modify jets resulting from collisions between nuclei. Calculations showed that a parton traversing a hot and dense medium consisting of other partons — that is, a quark–gluon plasma — should lose substantially more energy than one traversing cold nuclear matter[32–34]. This prediction appears to be borne out by data from all four experiments at RHIC.

A jet is much more difficult to see in a heavy-ion collision than after a collision between protons. The reason is the sheer number of particles produced: a single central (head-on) gold–gold collision generates about 5,000 charged particles, and unless the jet has very high (transverse) momentum, it will not stand out in the crowd. But the presence of jets will affect the overall transverse momentum distribution. At low transverse momenta, the spectrum in a heavy-ion collision is complex, as it is a superposition of hydrodynamic expansion effects and random thermal motion. Nevertheless, for particles of a particular species with transverse momenta that are significantly larger than their mass, the resulting spectrum is nearly exponential. The contribution of jets with high transverse momentum leads to a distinct power-law behaviour typically visible for values of transverse momentum of a few GeV or more.

To judge a possible modification of the shape of the spectrum in a high-energy nuclear collision, the transverse-momentum distribution of π mesons produced in central gold–gold collisions at RHIC can be compared with that measured in proton–proton collisions. To quantify this comparison, the ratio of the gold–gold-collision spectrum to the proton–proton-collision spectrum is scaled to the total number of inelastic collisions in the nuclear case, providing the suppression factor R_{AA}. For larger transverse momenta, this factor settles at about 0.2 (Fig. 4); that is, the production of high-momentum π mesons is suppressed by a factor of five in gold–gold collisions.

What is the origin of this suppression? The transverse-momentum spectrum for collisions between protons agrees well[35] with theoretical calculations that use next-to-leading-order quantum chromodynamic perturbation theory. When the spectra of deuteron–gold collisions of varying centrality are compared with the proton–proton spectrum, R_{AA} is 1 or larger (for more central collisions, values larger than 1 are even expected — a phenomenon known as the Cronin effect, caused by the scattering of partons before the hard collision). For peripheral gold–gold collisions, the values of R_{AA} also correspond well to the expectation from collisions between protons. The clear implication is that something special and new happens in central gold–gold collisions: the precursor parton of the jet produced must lose a lot of energy, causing the transverse-momentum spectrum of the mesons in the jet to fall off steeply.

Several researchers have shown that only calculations including large energy loss in the medium can account for these data. The clear implication is that the medium present in the collision fireball is hot and dense, and when partons pass through it, they lose energy. Both radiation of gluons and elastic scattering seem to be important here. In deuteron–gold collisions, by contrast, the jet sees at most cold nuclear matter (or a vacuum), and does not seem to be perturbed.

Calculating the energy loss of a fast parton in a quantum chromodynamic liquid, as suggested by the data discussed in the previous section, is beyond the current theoretical state-of-the-art. To gain insight into the underlying physics of energy loss, it is helpful to resort to another aspect of the medium: that it contains many gluons. Indeed, the RHIC data on parton energy loss are well explained by modelling the medium formed by the collision as an ultra-dense gluon gas with a density of the number of gluons (N_g) per rapidity interval of $dN_g/dy = 1{,}100$. Here, the rapidity y is a logarithmic measure of the gluon's longitudinal velocity, v. With the simple assumption that $v = z/t$ (z is the longitudinal space coordinate), Bjorken[36] showed how to map rapidity densities to spatial densities. The spatial gluon density in turn is linked directly to entropy density. Using relations from statistical mechanics for a relativistic gas of bosons (and fermions if quarks are included), the temperature and energy density can be obtained from these gluon densities. The high gluon densities needed to reproduce the observed gold–gold R_{AA} correspond to an initial temperature of about twice the critical temperature for the formation of a quark–gluon plasma. The initial energy densities of 14–20 GeV fm^{-3} are

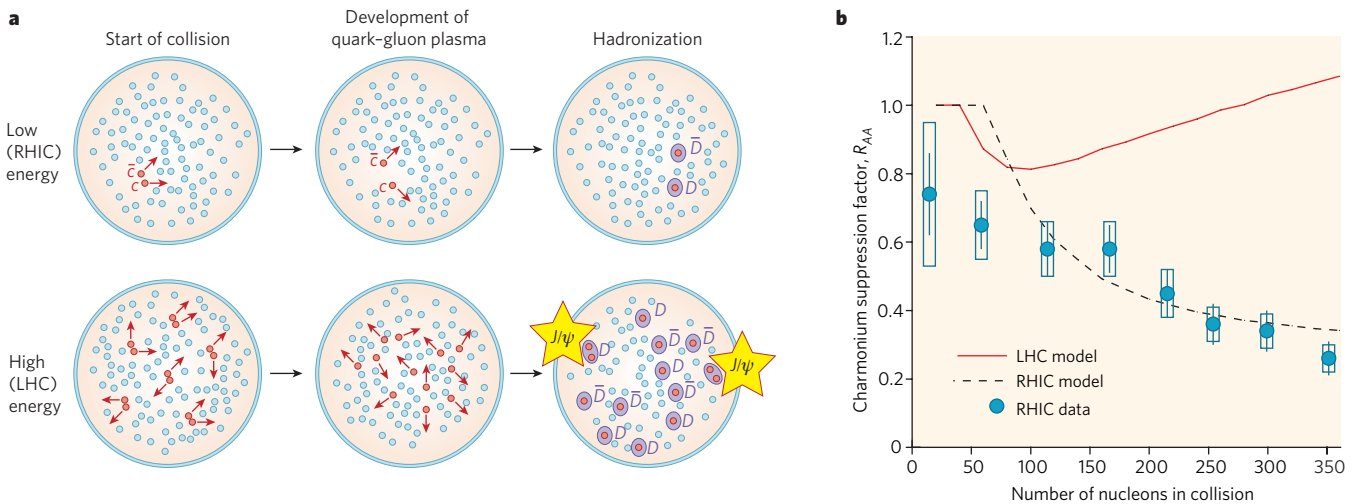

Figure 6 | Charmonium suppression. a, At low energies, the quark–gluon plasma screens interaction between the only pair of charm quark and antiquark produced (red dots) and any other two quarks (up, down, strange) will find themselves paired with the charm quark/antiquark in *D* mesons at hadronization (purple circles). At high energies, by contrast, many charm–anticharm pairs are produced in every collision and at hadronization, charm and anticharm quarks from different original pairs may combine to form a charmonium J/Ψ particle. Grey dots indicate light partons produced in the collision. **b,** Theory and experiment compared quantitatively. Model predictions[55] for the charmonium suppression factor agree well with recent RHIC data from the PHENIX collaboration[66]. Owing to the increased level of statistical recombination expected, enhancement rather than suppression is predicted for LHC conditions. What the experiments deliver will be a further crucial test of theories of the quark–gluon plasma. Part b reproduced, with permission, from ref. 55.

Box 1 | ALICE: the LHC's dedicated plasma hunter

LHC's ALICE detector is dedicated to investigating nucleus–nucleus collisions at an energy of 2.8 TeV per nucleon in each of the colliding nuclei. The main part of the apparatus is housed in the world's largest solenoidal magnet, which generates a field strength of 0.5 T within a volume of 1,600 m^3.

Various detectors arranged in cylindrical shells around the interaction point (see figure) are designed to determine the identity and precise trajectory of the more than 10,000 charged particles propelled by a lead–lead nuclear collision into the active volume of the apparatus. The innermost detector is the inner tracking system (ITS), which consists of six layers of silicon detectors surrounding the 1-mm-thick beam pipe that encloses the ultra-high vacuum of the accelerator. These detectors are capable of high-precision tracking (resolution around 20 μm) so as to determine the decay vertex of short-lived particles carrying strange, charm, or bottom quantum numbers that typically decay within a few millimetres to centimetres of the primary interaction point.

The ITS is contained within, and mounted on, the cylindrical barrel of the time projection chamber (TPC). This is ALICE's major tracking device: it is the largest of its kind worldwide, with some 560,000 readout channels, and provides essentially continuous, three-dimensional tracking of charged particles between radii of 80 cm and 250 cm from the central interaction point.

Outside the TPC are two very large (with areas of around 150 m^2) particle identification detectors: the transition radiation detector (TRD), with more than 1 million channels and an on-board computer farm of a quarter-million central processing units for the triggering and identifying of electrons; and surrounding this, the time-of-flight (TOF) detector which can record the transit time between the interaction point and the detector surface at a resolution of better than 100 picoseconds.

The central barrel of ALICE is completed by dedicated detectors to measure photons (PHOS) and their distribution in the forward direction (PMD) and to identify high-momentum hadrons (HMPID), and by

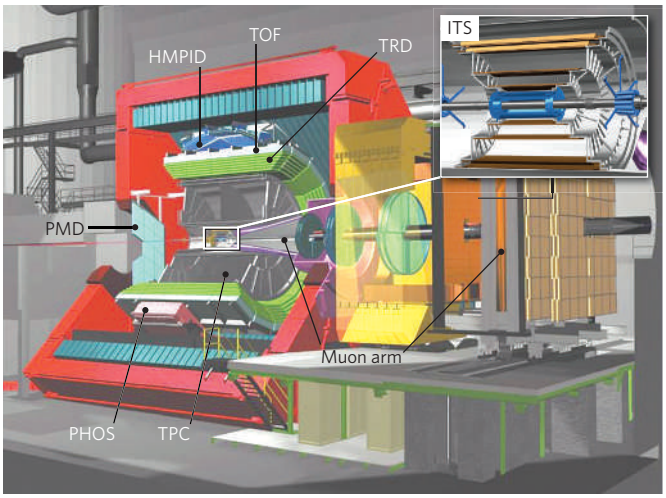

further detectors to determine the position and time of the primary interaction point. Separated from the main detector in the forward direction of one of the accelerator beams, and behind a conical absorber that projects into the central barrel, is a muon detector with its own large dipole magnet. Because muons do not undergo strong reactions, and because those at relevant energies do not emit *bremsstrahlung*, they penetrate the absorber practically unscathed — unlike hadrons. Their momenta are then measured in tracking stations before, inside, and after the dipole magnet.

The huge scale and cutting-edge engineering of the ALICE detector should allow it to make a decisive contribution to understanding the properties of the medium that will be created in the LHC's high-energy collisions between nuclei. Image courtesy of the ALICE collaboration.

also well in line with the initial conditions required by the hydrodynamic models introduced earlier. Both the temperature and the energy density are well above the critical conditions calculated with lattice quantum chromodynamics (Fig. 5).

Another important cross-check for the gluon-gas interpretation is to compare the transverse-momentum spectrum of photons produced in hard initial parton scattering in gold–gold and in proton–proton collisions. For most values of transverse momentum, the corresponding R_{AA} factors are consistent with unity (Fig. 4). This is perfectly in line with an unmodified distribution as produced in initial hard scattering: the photon does not participate in the strong force, and so would traverse a gluon-dominated fireball without further interaction.

Similar analyses have been done for several different hadronic species. Generally, within the errors, all mesons behave just like π mesons (the data points for η mesons are shown in Fig. 4). In an intermediate range of 2–6 GeV, the suppression of baryons is significantly weaker, but for high transverse momentum it joins that for π mesons.

Another characteristic of hadron jets is the back-to-back correlation of two of them in the plane perpendicular to the colliding beams. Even without reconstructing the jet (the difficulty of doing this in a heavy-ion collision has been mentioned), such an analysis can be done by selecting just the particles that have the highest momentum in an event. Both the PHENIX and STAR experiments have undertaken such a 'leading particle' analysis, picking just one high-transverse-momentum trigger particle (say, in the range 4–6 GeV) and then checking for the distribution in azimuthal angle of all other 'associated' particles in a given range of transverse momenta. Proton–proton experiments produce two peaks, one at 0° and one at 180°. This is expected, as the associated particle could be a fragment of the same jet (the 0° peak), or a leading particle of the second jet diametrically opposite (the 180° peak).

In gold–gold collisions, a dramatic change is seen[37,38] when the transverse momentum of the associated particle is varied. At very high momenta, the two expected peaks are present. For lower particle momenta (2–4 GeV), however, the peak at 180° broadens to the point that it is barely visible. For even lower momenta, it develops into a dip with two pronounced peaks, one on either side about 1 radian apart. A very similar observation has been made at the top SPS energy[39,40]. The interpretation of this feature of the data is still hotly debated, but an interesting suggestion has been made[41,42]: the dip with the two satellite peaks could indicate the presence of a shock wave in the form of a Mach cone caused by a supersonic parton traversing the quark–gluon plasma. If borne out, this could lead to the determination of the speed of sound in the plasma.

The modelling of the parton energy loss in the quark–gluon plasma is still somewhat schematic, and leaves open a range of theoretical possibilities and ways of implementation. To sharpen the interpretation, it would be good to have individual measurements of the properties of jets stemming from all different quark flavours, as well as from gluons. For heavy quarks (charm and bottom), an important step has been made by the PHENIX and STAR collaborations at RHIC. Both experiments have measured transverse-momentum spectra of electrons stemming from decays of D and B mesons (each of which contain a charm or bottom quark) into electrons plus anything else. The R_{AA} values have been determined for these spectra[43,44], too, and have been surprising: they are very close to the values determined for mesons that involve only up, down and strange quarks. Theoretically, energy loss by radiation should be much lower for the charm and bottom quarks than for the up, down and strange quarks and gluons owing to their much larger masses. Since then, it has been realized that energy loss by scattering is probably of comparable importance to energy loss by radiation[45,46], which improves the quantitative situation somewhat, but doesn't resolve the puzzle.

With the start of experiments at the LHC, matters will change dramatically: because of the much higher beam energy, jet production will be enhanced by many orders of magnitude compared with the situation at RHIC energy. Estimates[47] based on solving quantum chromodynamics by perturbation theory imply, for example, an enhancement of

more than four orders of magnitude at $p_t = 100$ GeV. Thus a whole new range of transverse-momentum values between 20 and 250 GeV will become accessible. Such measurements can then be used to discriminate between the various theoretical scenarios competing to describe parton energy loss, either by determination of R_{AA} or, uniquely for the LHC, by direct reconstruction of the jet in a collision between nuclei. This should allow jet probes to be developed into quantitative tools to determine the parton density of the matter formed.

Charmonia as harbingers of deconfinement?

The particles collectively known as charmonia — bound states of heavy charm quarks and antiquarks — have a special role in research into the quark–gluon plasma. In 1986, Satz and Matsui[48] realized that the high density of gluons in a quark–gluon plasma should destroy charmonium systems, in a process analogous to Debye screening of the electromagnetic field in a plasma through the presence of electric charges. The suppression of charmonia (compared with their production in the absence of a quark–gluon plasma) was thus proposed as a 'smoking gun' signature for plasma formation in nuclear collisions at high energy. Measurements at the SPS[49] did indeed provide evidence for such suppression in central collisions between heavy nuclei. No suppression was found in grazing collisions or in collisions between light nuclei, in which a plasma is not expected to form. But absorption of charmonium in the nuclear medium, as well as its break-up by hadrons produced in the collision, is also a mechanism that could lead to charmonium suppression even in the absence of plasma formation[50], and the interpretation of the SPS data remains inconclusive.

This situation took an interesting turn in 2000, when researchers realized that the large number of charm-quark pairs produced in nuclear collisions at collider energies could lead to new ways to produce charmonium, either through statistical production at the phase boundary[51,52], or through coalescence of charm quarks in the plasma[53]. At low energy, the mean number of charm-quark pairs produced in a collision is much fewer than 1, implying that charmonium is formed, if at all, always from charm quarks of this one pair. Because the number of charm quarks in a collision at LHC energy is expected to reach about 200, charm quarks from different pairs can combine to form charmonium (Fig. 6a). This works effectively only if a charm quark can travel a substantial distance in the plasma to 'meet' its prospective partner. Under these conditions, charmonium production scales quadratically with the number of charm-quark pairs, so enhancement, rather than strong suppression, is predicted for LHC energy[54,55] (Fig. 6b). If observed, this would be a spectacular fingerprint of a high-energy quark–gluon plasma, in which charm quarks are effectively deconfined. Again, as in most other cases, the data from the LHC will be decisive in settling the issue.

Looking forward

The data from the SPS and particularly the RHIC accelerator have taught us that central nuclear collisions at high energy produce a medium made up of partonic matter in equilibrium and possessing collective properties. The medium flows much like an ideal liquid and is dense enough to dissipate most of the energy of a 20 GeV parton. Future experiments at RHIC will further elucidate some of the aspects discussed above, in particular in the heavy-quark sector. With their 30 times higher energy, lead–lead collisions at LHC in the specially designed ALICE detector (Box 1) will produce this new state of matter at unprecedented energy densities and temperatures and over very large volumes compared with the size of the largest stable nuclei. With the planned experiments, the LHC heavy-ion community looks forward with anticipation to elucidating the properties of such partonic fireballs. The prize is unravelling the mystery of the matter that formed a fraction of a nanosecond after the Big Bang, and disappeared just 10 microseconds later. ■

1. Gross, D. J. & Wilczek, F. Ultraviolet behavior of non-abelian gauge theories. *Phys. Rev. Lett.* **30,** 1343–1346 (1973).
2. Politzer, H. J. Reliable perturbative results for strong interactions? *Phys. Rev. Lett.* **30,** 1346–1349 (1973).
3. Cabibbo, N. & Parisi, G. Exponential hadronic spectrum and quark liberation. *Phys. Lett. B* **59,** 67–69 (1975).
4. Collins, J. C. & Perry, M. J. Superdense matter: neutrons or asymptotically free quarks? *Phys. Rev. Lett.* **34,** 1353–1356 (1975).
5. Hagedorn, R. Statistical thermodynamics of strong interactions at high energies. *Nuovo Cimento Suppl.* **3,** 147–186 (1965).
6. Karsch, F., Laermann, E. & Peikert, A. Quark mass and flavour dependence of the QCD phase transition. *Nucl. Phys. B* **605,** 579–599 (2001).
7. Aoki, A., Fodor, Z., Katz, S. D. & Szabo, K. K. The QCD transition temperature: results with physical masses in the continuum limit. *Phys. Lett B.* **643,** 46–54 (2006).
8. Fodor, Z. & Katz, S. Critical point of QCD at finite T and μ, lattice results for physical quark masses. *J. High Energy Phys.* **4,** 050 (2004).
9. Allton, C. R. *et al.* The QCD thermal phase transition in the presence of a small chemical potential. Preprint at <http://arxiv.org/abs/hep-lat/0204010> (2002).
10. Ejiri, S. *et al.* Study of QCD thermodynamics at finite density by Taylor expansion. Preprint at <http://arxiv.org/abs/hep-lat/0312006> (2003).
11. CERN. New state of matter created at CERN. <http://press.web.cern.ch/press/PressReleases/Releases2000/PR01.00EQuarkGluonMatter.html> (2000).
12. Heinz, U. & Jacob, M. Evidence for a new state of matter: an assessment of the results from the CERN lead beam programme. Preprint at <http://arxiv.org/abs/nucl-th/0002042> (2000).
13. Arsene, I. *et al.* Quark–gluon plasma and color glass condensate at RHIC? The perspective from the BRAHMS experiment. *Nucl. Phys. A* **757,** 1–27 (2005).
14. Back, B. B. *et al.* The PHOBOS perspective on discoveries at RHIC. *Nucl. Phys. A* **757,** 28–101 (2005).
15. Adams, J. *et al.* Experimental and theoretical challenges in the search for the quark–gluon plasma: the STAR Collaboration's critical assessment of the evidence from RHIC collisions. *Nucl. Phys. A* **757,** 102–183 (2005).
16. Adcox, K. *et al.* Formation of dense partonic matter in relativistic nucleus–nucleus collisions at RHIC: experimental evaluation by the PHENIX Collaboration. *Nucl. Phys. A* **757,** 184–283 (2005).
17. Csörgö, T., Dávid, G., Lévai. P. & Papp, G. (eds) Quark matter 2005 — proceedings of the 18th international conference on ultra-relativistic nucleus–nucleus collisions. *Nucl. Phys. A* **774,** 1–968 (2006).
18. Andronic, A., Braun-Munzinger, P. & Stachel, J. Hadron production in central nucleus–nucleus collisions at chemical freeze-out. *Nucl. Phys. A* **772,** 167–199 (2006).
19. Becattini, B., Gadzicki, M., Keranen, A., Manninen, J. & Stock, R. Chemical equilibrium study in nucleus–nucleus collisions at relativistic energies. *Phys. Rev. C* **69,** 024905 (2004).
20. Braun-Munzinger, P., Redlich, K. & Stachel, J. in *Quark–Gluon Plasma 3* (eds Hwa, R. C. & Wang, X. N.), 491–599 (World Scientific, Singapore, 2004).
21. Braun-Munzinger, P. & Stachel, J. Probing the phase boundary between hadronic matter and the quark-gluon plasma in relativistic heavy-ion collisions. *Nucl. Phys. A* **606,** 320–328 (1996).
22. Braun-Munzinger, P., Stachel, J. & Wetterich, C. Chemical freeze-out and the QCD phase transition temperature. *Phys. Lett. B.* **596,** 61–69 (2004).
23. Stock, R. The parton to hadron phase transition observed in Pb+Pb collisions at 158 GeV per nucleon. *Phys. Lett. B* **456,** 277–282 (1999).
24. Heinz, U. Hadronic observables: theoretical highlights. *Nucl. Phys. A* **638,** c357–364 (1998).
25. Aoki, Y., Fodor, Z., Katz, S. D. & Szabo, K. K. The order of the quantum chromodynamics transition predicted by the standard model of particle physics. *Nature* **443,** 675–678 (2006).
26. Gyulassy, M. & McLerran, L. New forms of QCD matter discovered at RHIC. *Nucl. Phys. A* **750,** 30–63 (2005).
27. Baier, R., Romatschke, P. Causal viscous hydrodynamics for central heavy-ion collisions. Preprint at <http: //arxiv.org/nucl-th/0610108> (2006).
28. Romatschke, P. Causal viscous hydrodynamics for central heavy-ion collisions II: meson spectra and HBT radii. Preprint at <http://arxiv.org/nucl-th/0701032> (2007).
29. Heinz, U., Song, H. & Chaudhuri, A. K. Dissipative hydrodynamics for viscous relativistic fluids. *Phys. Rev. C* **73,** 034904 (2006).
30. Bhalerao, R. S., Blaizot, J. P., Borghini, N. & Ollitrault, J. Y. Elliptic flow and incomplete equilibration at RHIC. *Phys. Lett. B* **627,** 49–54 (2005).
31. Bjorken, J. D. Fermilab-PUB-82-59-THY (1982) and erratum (unpublished).
32. Wang, X. N. & Gyulassy, M. Gluon shadowing and jet quenching in *A+A* collisions at $\sqrt{s} = 200A$ GeV. *Phys. Rev. Lett.* **68,** 1480–1483 (1992).
33. Baier, H., Dokshitzer, Y. L., Mueller, A. H., Peigne, S. & Schiff, D. Radiative energy loss of high energy quarks and gluons in a finite-volume quark-gluon plasma. *Nucl. Phys. B* **483,** 291–320 (1997).
34. Baier, H., Dokshitzer, Y. L., Mueller, A. H., Peigne, S. & Schiff, D. Radiative energy loss and $p_\perp$-broadening of high energy partons in nuclei. *Nucl. Phys. B* **484,** 265–282 (1997).
35. d'Enterria, D. Quantum chromo (many-body) dynamics probed in the hard sector at RHIC. Preprint at <http://arxiv.org/abs/nucl-ex/0406012> (2004).
36. Bjorken, J. D. Highly relativistic nucleus–nucleus collisions: the central rapidity region. *Phys. Rev. D* **27,** 140–151 (1983).
37. Adler, S. S. *et al.* (PHENIX collaboration). A detailed study of high-p_T neutral pion suppression and azimuthal anisotropy in Au+Au Collisions at $\sqrt{s_{NN}} = 200$ GeV. Preprint at <http://arxiv.org/abs/nucl-ex/0611007> (2006).
38. Mischke, A. (for the STAR collaboration). High-p_T hadron production and triggered particle correlations. Preprint at <http://arxiv.org/abs/nucl-ex/0605031> (2006).
39. Adamova, D. *et al.* (CERES collaboration). Semihard scattering unraveled from collective dynamics by two-pion azimuthal correlations in 158*A* GeV/*c* Pb+Au collisions. *Phys. Rev. Lett.* **92,** 032301 (2004).
40. Ploskon, M. (for the CERES collaboration). Two particle azimuthal correlations at high transverse momentum in Pb–Au at 158 A GeV/c. Preprint at <http://arxiv.org/abs/nucl-ex/0701023nucl-ex/0701023> (2007).
41. Stöcker, H. Collective flow signals the quark–gluon plasma. *Nucl. Phys. A* **750,** 121–147 (2005).

42. Casalderrey-Solana, J., Shuryak, E. & Teaney, D. Conical flow induced by quenched QCD jets. Preprint at <http://arxiv.org/abs/hep-ph/0411315> (2004).
43. Adare, A. *et al.* (the PHENIX collaboration). Energy loss and flow of heavy quarks in Au+Au collisions at $\sqrt{s_{NN}}$ = 200 GeV. Preprint at <http://arxiv.org/abs/nucl-ex/0611018> (2006).
44. Zhang, H. *et al.* Heavy flavour production at STAR. *J. Phys. G* **32,** S29–S34 (2006).
45. Zapp, K., Ingelman, G., Rathmans, J. & Stachel, J. Jet quenching from soft QCD scattering in the quark–gluon plasma. *Phys. Lett. B.* **637,** 179–184 (2006).
46. Adil, A., Gyulassy, M., Horowitz, W. A. & Wicks, S. Collisional energy loss of non asymptotic jets in a QGP. Preprint at <http://arxiv.org/abs/nucl-th/0606010> (2006).
47. Vitev, I. Contribution to CERN yellow report on hard probes in heavy ion collisions at the LHC. Preprint at <http://arxiv.org/abs/hep-ph/0310274> (2003).
48. Satz, H. & Matsui, T. J/ψ suppression by quark-gluon plasma formation. *Phys. Lett. B* **178,** 416–422 (1986).
49. Abreu. M. C. *et al.* Transverse momentum distributions of $J/\psi, \psi'$. Drell–Yan and continuum dimuons produced in Pb–Pb interactions at the SPS. *Phys. Lett. B* **499,** 85–96 (2001).
50. Capella, A., Kaidalov, A. B. & Sousa, D. Why is the J/ψ suppression enhanced at large transverse energy? *Phys. Rev. C* **65,** 054908 (2002).
51. Braun-Munzinger, P. & Stachel, J. (Non)thermal aspects of charmonium production and a new look at J/ψ suppression *Phys. Lett. B* **490,** 196–202 (2000).
52. Braun-Munzinger, P. & Stachel, J. On charm production near the phase boundary. *Nucl. Phys. A* **690,** 119–126 (2001).
53. Thews, R. L., Schroedter, M. & Rafelski, J. Enhanced J/ψ production in deconfined quark matter. *Phys. Rev. C* **63,** 054905 (2001).
54. Andronic, A., Braun-Munzinger, P., Redlich, K. & Stachel, J. *Nucl. Phys. A.* Preprint at <http://arxiv.org/abs/nucl-th/0611023> (2006).
55. Andronic, A., Braun-Munzinger, P., Redlich, K. & Stachel, J. *Phys. Lett. B.* Preprint at <http://arxiv.org/abs/nucl-th/0701079> (2007).
56. Barrette, J. *et al.* Observation of anisotropic event shapes and transverse flow in Au–Au collisions at AGS energy. *Phys. Rev. Lett.* **73,** 2532–2536 (1994).
57. Voloshin, S. & Zhang, Y. C. Flow study in relativistic nuclear collisions by Fourier expansion of azimuthal particle distributions. *Z. Phys. C* **70,** 665–671 (2007).
58. Poskanzer, A. M & Voloshin, S. A. Methods for analyzing anisotropic flow in relativistic nuclear collisions. *Phys. Rev. C* **58,** 1671–1678 (1998).
59. Huovinen, P. *et al.* Radial and elliptic flow at RHIC: further predictions. *Phys. Lett. B* **503,** 58–64 (2001).
60. Teaney, D., Lauret, J. & Shuryak, E. A hydrodynamic description of heavy ion collisions at the SPS and RHIC. Preprint at <http://arxiv.org/abs/nucl-th/0110037> (2001).
61. Kolb, P. & Heinz, U. in *Quark–Gluon Plasma 3* (eds Hwa, R. C. & Wang, X. N.) 634–714 (World Scientific, Singapore, 2004).
62. Adams, J. *et al.* (the STAR collaboration). Azimuthal anisotropy in Au+Au collisions at $\sqrt{s_{NN}}$ = 200 GeV. *Phys. Rev.* **C72,** 014904 (2005).
63. Vitev, I. Jet quenching in relativistic heavy ion collisions *J. Phys. G.* Preprint at <http://arxiv.org/abs/hep-ph/0503221> (2005).
64. Akiba, Y. Probing the properties of dense partonic matter at RHIC. *Nucl. Phys. A* **774,** 403–408 (2006).
65. Kolb, P. & Heinz, U. in *Quark–Gluon Plasma 3* (eds Hwa, R. C. & Wang, X. N.) 1–59 (World Scientific, Singapore, 2004).
66. Adare, A. *et al.* (PHENIX collaboration). J/ψ production vs centrality, transverse momentum, and rapidity in Au+Au collisions at $\sqrt{s_{NN}}$ = 200 GeV. Preprint at <http://arxiv.org/abs/nucl-ex/0611020nucl-ex/0611020> (2006).

Author Information Reprints and permissions information is available at npg.nature.com/reprintsandpermissions. The authors declare no competing interests. Correspondence should be addressed to J.S. (stachel@physi.uni-heidelberg.de).